Mineralogy and Petrology (2023) 117:133–143
https://doi.org/10.1007/s00710-022-00808-9

RESEARCH

$K[(Cu^{II},Mn^{II},Mn^{III})_2(TeO_3)_3]\cdot 2H_2O$, the first zemannite-type structure based on a Jahn-Teller-distorted framework

Felix Eder[1] · **Ronald Miletich**[2] · **Matthias Weil**[1]

Received: 31 October 2022 / Accepted: 22 December 2022 / Published online: 18 March 2023

Abstract

Synthetic single crystals of $K[(Cu^{II},Mn^{II},Mn^{III})_2(TeO_3)_3]\cdot 2H_2O$ were obtained from an overconcentrated alkaline aqueous solution in the system K_2O-MnO-CuO-TeO_2 under hydrothermal conditions at $T \leq 220$ °C. Subeuhedral single crystals have been investigated by means of single-crystal X-ray diffraction. The crystal structure of this new zemannite-type representative adopts a monoclinic twofold superstructure. The doubling of the unit-cell volume is accompanied by a hexagonal-to-monoclinic symmetry reduction, resulting in threefold twinning with individual crystal domains following the space group symmetry $P2_1$. Refinements of site-occupation factors and the evaluation of bond valences suggest a distribution of di- and trivalent cations at the octahedrally coordinated *M* sites with a ratio $(Cu^{II} + Mn^{II}):Mn^{III}$ approximating 1:1. Based on arguments about the cation sizes and the individual bond valence sums, a distribution of $Cu^{II}_{1-x}Mn^{III}_{x}$ and $Mn^{II}_{x}Mn^{III}_{1-x}$ at each two of the four *M* sites can be assumed with *x* between ~ 0.14 and ~ 0.50. The K^+ cations and H_2O molecules inside the channels are located off the central channel axis. In contrast to most other known zemannite-type phases, the extra-framework atoms show full occupancies and are not disordered. The distribution of the channel contents supports the anisotropic deformation of the surrounding framework, which follows the local symmetry reduction as required for the Jahn-Teller distortion of the octahedrally coordinated *M* sites within the framework. The arrangement of the deformed channels can be understood as the origin of the existing superstructure.

Keywords Oxidotellurate(IV) · Zemannite · Crystal structure · Cation ordering · Low-symmetry superstructure · Twinning

Introduction

The zemannite structure type was reported for the first time in connection with structural studies of the rare mineral zemannite, described as a new species from the Moctezuma mine in Mexico, originally assuming the composition $Na_xH_{2-x}[(Zn^{II},Fe^{III})_2(TeO_3)_3]\cdot yH_2O$ (Matzat 1967; Mandarino et al. 1969). Based on crystal structure and crystallochemical investigations, the composition of zemannite was revised subsequently to the idealized formula $Mg_{0.5}[Zn^{II}Fe^{III}(TeO_3)_3]\cdot 4.5H_2O$ (Miletich 1995a). Crystal structure determinations of the minerals kinichilite (Hori et al. 1981), ilirneyite (Pekov et al. 2018) and keystoneite (Missen et al. 2021) reveal those minerals to be isostructural to zemannite. Its crystal structure represents a channel structure, with Mg^{2+} cations and H_2O molecules occupying the extra-framework sites inside enclosed channels.

During the 1990s, first synthetic zemannite-type phases moved into the spotlight of research, as exemplified by the oxidoselenates(IV) $K_2[Co^{II}_2(SeO_3)_3]\cdot 2H_2O$ and $K_2[Ni^{II}_2(SeO_3)_3]\cdot 2H_2O$ (Wildner 1993), and the oxidotellurates(IV) $Na_2[Co^{II}_2(TeO_3)_3]\cdot 3H_2O$ and $Na_2[Zn^{II}_2(TeO_3)_3]\cdot 3H_2O$ (Miletich 1995b). Pioneering work produced various new oxidoselenates(IV) and -tellurates(IV) with Na^+, K^+, and Ba^{2+} cations in the channels, and even examples revealing neutral frameworks and empty channels have been reported (Wontcheu and Schleid 2003; Kong et al. 2010; Johnston and Harrison 2011). The first synthetic zemannite-type phases containing more than one transition metal cation, with compositions of $Na_x[Fe^{III}_{2-x}$

Editorial handling: T. Armbruster

✉ Felix Eder
felix.eder@tuwien.ac.at

[1] Institute of Chemical Technologies and Analytics, Division of Structural Chemistry, Technical University of Vienna, Getreidemarkt 9/164-SC, A-1060 Vienna, Austria

[2] Department of Mineralogy and Crystallography, University of Vienna, Josef-Holaubek-Platz 2, A-1090 Vienna, Austria

$Zn^{II}_{x}(TeO_3)_3]\cdot 3H_2O$ ($0.55 \leq x \leq 1.25$), were synthesized by Missen et al. (2019a). Most recently, several novel representatives of zemannite-type phases, partially with formation of superstructures and/or symmetry reductions, were described by Eder et al. (2023).

Within the scope of systematic experimental work aiming at the synthesis of novel analogous oxidotellurate(IV) phases, hydrothermal syntheses have been performed on various transition-metal bearing systems using alkaline solutions almost 30 years ago (Miletich 1993a). Among them, series of formation studies were conducted in the system K_2O-MnO-CuO-TeO_2 with targeting at novel microporous oxidotellurates(IV) adopting the denningite or zemannite structure. Both structure types are characterized by isolated channels within a framework composed of transition metals and Te^{IV} in O-based coordination. Individual synthesis experiments resulted in an unexpected loss of water due to inappropriate sealing of the reaction containers, so that K-bearing oxidotellurates(IV) could form from the overconcentrated alkaline hydrothermal solutions. In this context, $K_2[Zn_2(TeO_3)_3]\cdot 3H_2O$ and $K[(Mn,Cu)_2(TeO_3)_3]\cdot nH_2O$ were coincidently obtained as compounds structurally related to zemannite, but their crystal structures have not yet been determined. In the case of $K_2[Zn_2(TeO_3)_3]\cdot 3H_2O$, it was due to the lack of suitable untwinned crystals, as powder diffraction measurement indicated a monoclinic unit-cell as derived from peak splitting. Following our most recent findings on novel synthetic zemannite-type phases (Eder et al. 2023), it was possible to grow crystals of a less hydrated K-Zn-zemannite phase (*i.e.* $K_2[Zn_2(TeO_3)_3]\cdot 2H_2O$), which, however, was found to be metrically hexagonal and not monoclinic.

Nevertheless, the preliminary investigations on the K-(Cu,Mn)-zemannite phase by means of X-ray film techniques (Miletich 1993a) clearly revealed twinning by non-merohedry of non-hexagonal lattice domains. It was deduced that the crystal structure of this K-(Cu,Mn)-zemannite has a unit-cell with twice the size of the usual hexagonal zemannite basic cell ($a \approx 9.3$ Å, $c \approx 7.7$ Å), showing a doubling of one of the *a*-axes and thus leading to a symmetry reduction, which most likely corresponds to the monoclinic system. At that time, the appearance of the superimposing threefold twinned pseudohexagonal domains was a distinct limit for diffractometry, which in this case inhibited any successful attempt to solve the crystal structure. All that remained, was the unverified assumption that the deviation from the original hexagonal symmetry, and thus the distortion of the lattice in this particular zemannite, is probably due to the Jahn-Teller effects of the Cu^{II} and Mn^{III} cations, which are incompatible with the site symmetry in the parental $P6_3/m$ symmetry of the archetype framework.

On the occasion of the 100th anniversary of the birthday of Prof. Josef Zemann (1923–2022), after whom the mineral was named and who is therefore the namesake of this structural family, we decided to determine the crystal structure of the $K[(Cu,Mn)_2(TeO_3)_3]\cdot nH_2O$ ($n \approx 2$) zemannite phase with a modern CCD-based diffractometer to resolve the problems related to an apparent symmetry reduction. The upcoming anniversary was motivating to us in that Prof. Zemann was not only a pioneer in the structural chemistry of oxidotellurates(IV) (Zemann 1968, 1971, 1974), but also dealt with the peculiar crystal chemistry of mineral structures with Jahn-Teller-active cations, especially Cu^{II}, in countless examples (*e.g.* Gattow and Zemann 1958).

Experimental

Synthesis

Single crystals of $K[(Cu^{II},Mn^{II},Mn^{III})_2(TeO_3)_3]\cdot 2H_2O$ were obtained from experiments under hydrothermal conditions originally aiming at the synthesis of Cu-substituted denningite-type $(Cu,Mn)Te_2O_5$ phases (Miletich 1993b). A stoichiometric mixture of 0.128 g $MnCl_2\cdot 4H_2O$, 0.211 g $CuCl_2\cdot 2H_2O$ and 0.621 g TeO_2, corresponding to the molar ratio 1 Mn:2 Cu:6 Te, was placed inside a Teflon-lined steel autoclave. The reaction container measuring ~ 4.5 to 5 cm^3 in volume was filled with water and concentrated KOH solution in such a way that a pH value of 9.5 was achieved at a filling level of about 70%. Then the mechanically sealed autoclave was heated to 220 °C and kept at this temperature under autogenous pressure for 92 h. When opening the autoclave after cooling to room temperature, it was observed that the filling level of the hydrothermal fluid had significantly decreased from more than two thirds to ~ 20%. The insufficiently closed autoclave inadvertently led to high fluid losses in this specific experiment, so that an exceptionally high concentration of the K contents, which are otherwise preferred to fractionate into the remaining fluid phase, led to the crystallization of a K-containing oxidotellurate(IV) phase as a unique by-product.

The crystalline reaction products of this run (Fig. 1) were identified as a mixture of a denningite-type (Walitzi 1965) solid solution of composition $Mn^{II}(Mn^{II}_{0.18}Cu^{II}_{0.82})(Te_2O_5)_2$, minor amounts of spiroffite, $Mn^{II}_2Te_3O_8$ (Cooper and Hawthorne 1996) and rayite, $Cu^{II}Te_2O_5$ (Hanke et al. 1973), and subordinate amounts of the title compound $K[(Cu^{II},Mn^{II},Mn^{III})_2(TeO_3)_3]\cdot 2H_2O$, as identified by means of X-ray powder and single crystal diffraction. The subeuhedral K-(Cu,Mn)-zemannite crystals are characterized by an intensive dark brown colour and exhibit large hexagonal pillars up to 0.5 mm in length, morphologically dominated by the faces of the hexagonal prism.

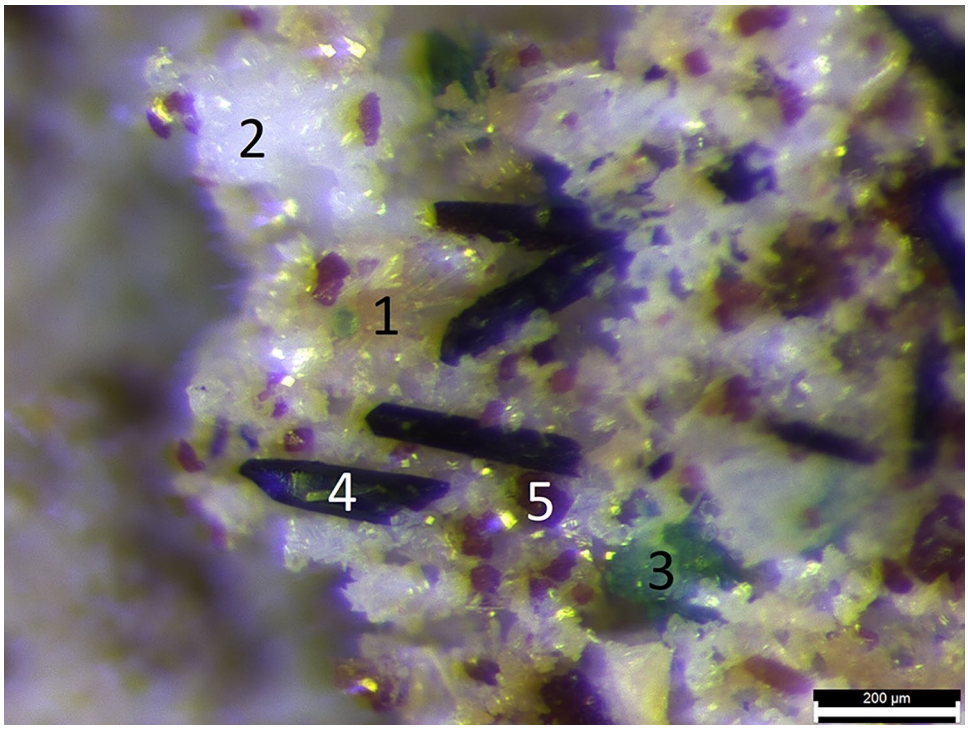

Fig. 1 The crystalline reaction products present in the original sample: $Mn^{II}(Mn^{II}_{0.18}Cu^{II}_{0.82})(Te_2O_5)_2$ (Miletich 1993b, yellow, 1), $Mn^{II}_2Te_3O_8$ (Cooper and Hawthorne 1996, colourless, 2), $Cu^{II}Te_2O_5$ (Hanke et al. 1973, green, 3) and the title compound $K[(Cu^{II},Mn^{II},Mn^{III})_2(TeO_3)_3]\cdot 2H_2O$ (dark brown, 4). The light brown crystals probably originate from minor amounts of α-$MnTeO_3$ (Trömel and Schmid 1972, 5)

X-ray diffraction measurement and refinement

Single crystal X-ray diffraction measurements were conducted on a Bruker Kappa Apex-II diffractometer using graphite-monochromatized MoK_α radiation and a CCD area detector. Data sets were recorded based on ω- and φ-scans (0.5° per frame, 30 s exposure time per frame), in the range $2.55° < 2\vartheta < 61.0°$ for the reciprocal space covering $\pm h \pm k \pm l$ (with $h \leq 13$, $k \leq 11$, $l \leq 22$). Details of the data collection and the crystal specimen used for the measurement are summarized in Table 1. Calculation of measurement strategies and integration were carried out with the instrument software APEX-4 (Bruker 2021a) and SAINT (Bruker 2021b), absorption correction with SADABS (Krause et al. 2015); the structure solution was achieved with SHELXT (Sheldrick 2015a), and the subsequent refinements performed with SHELXL 2018/3 (Sheldrick 2015b). Four reflections (101, $\bar{1}01$, 002, 201) appearing at the lowermost diffraction-angle range were omitted from the refinement as their intensities were significantly influenced by shadowing of the primary beam stop. For structure refinement, threefold twinning with the twin law

$$\begin{pmatrix} \overline{1/2} & 0 & 1/2 \\ 0 & 1 & 0 \\ \overline{3/2} & 0 & \overline{1/2} \end{pmatrix}$$

was considered using a hklf-5-type file comprising intensity data of separated and overlapping reflections of the three domains. Merging of the reflections during scaling in SADABS (Krause et al. 2015) led to smaller k and l ranges in the hkl file, as Friedel pairs were averaged. Since the final crystal structure model is non-centrosymmetric, it was also tried to suppress merging of Friedel pairs, thus resulting in six twin domains. However, the fractions of these additional three twin domains always resulted in negative values and corresponding refinement attempts did not converge appropriately. Therefore, all further refinements were carried out based on the data reduction with the above-mentioned threefold twinning.

The corresponding twin fractions were refined to values of 0.4256(16), 0.3223(16) and 0.2521(16), thus proving the suspected triplication of somewhat equal proportions of crystal domains. Apart from this twin triplication due to the parental pseudohexagonal arrangement, many reflections, which can be ascribed to only one of the three domains, still show a weak further splitting (Fig. 2a). This could be an indication of a further reduction in symmetry, possibly giving evidence of a weak triclinic distortion as manifested by the observed faint splitting. This feature has not been observed for the preliminary investigations carried out by precession photograph techniques 30 years ago (Fig. 2b). As this further splitting of the reflections is rather small and cannot be resolved properly for separate integration, it was ignored for any further consideration within the scope of this study.

The crystal structure was determined by means of direct methods as employed by the algorithm of SHELXT thus providing fractional coordinates corresponding to those transformed by the

Table 1 Data collection and refinement details

Empirical formula	$KCu_{0.73}Mn_{1.27}Te_3O_{11}H_4$
Structural formula	$K[(Cu_{0.73}Mn_{0.27})Mn(TeO_3)_3]\cdot 2H_2O$
M_R	718.11
Measurement T / K	296
Radiation λ / Å	MoK_α; 0.71073
Diffractometer	Bruker APEX-II
Crystal dimensions / mm^3	$0.23\times0.08\times0.08$
Space group, No	$P2_1$, 4
Formula units Z	4
a / Å	9.3857(13)
b / Å	7.6381(10)
c / Å	15.746(2)
β / °	90.464(4)
V / $Å^3$	1128.8(3)
μ / mm^{-1}	10.808
X-ray density / $g\times cm^{-3}$	4.202
θ_{min}–θ_{max} / °	2.969–30.458
h	–13—13
k	0—11
l	0—22
Independent reflections	3331
Observed reflections ($I>2\sigma(I)$)	2987
R_i	0.0489
Absorption correction	multiscan, SADABS (Krause et al. 2015)
Absorption T_{min}; T_{max}	0.1328; 0.2657
Parameters	200
Twin fractions	0.4256(16), 0.3223(16), 0.2521(16)
Flack parameter	0.04(6)
$R1$ ($F^2>2\sigma(F^2)$)	0.0407
$wR2$(F^2 all)	0.1018
GOF	1.077
Deposition code	CSD-2216656

$$\begin{pmatrix} \overline{1/2} & 1 & 0 \\ 0 & 0 & 1 \\ 1/2 & 0 & 0 \end{pmatrix}$$

matrix relative to positions given by Miletich (1995b).

Structure refinement attempts in the non-centrosymmetric space group $P2_1$ exhibited some issues, because the entire crystal structure exhibits $P2_1/m$ as a pseudosymmetry, which is only violated through the occupational distribution of the M atoms at their sites. Therefore, the y coordinates and the U^{12} and U^{23} values of the anisotropic displacement parameters (ADPs) of the atoms, which are located at sites sitting on the supposed m mirror plane in $P2_1/m$, did not converge properly. The corresponding y/b positional parameters consistently indicated to prefer equally two nearby positions close to the ideal mirror symmetry and did not achieve convergence even after hundreds of refinement cycles. This behaviour was suppressed by application of a stronger dampening term to the refinement using the DAMP command in SHELXL (Sheldrick 2015b). Moreover, the symmetry reduction led to larger correlations between pairs of positions related by the missing $m_{[010]}$ plane. Other than in $P2_1/m$, the O atoms could not be refined with ADPs in $P2_1$ because of negative values for several atoms. The final refinements were carried out in $P2_1$ space group symmetry using isotropic displacement parameters for all O atoms. Particular attention was also paid to the distribution of Mn and Cu atoms at the M positions, as well as the occupancy of K in the channels with regard to the variable distribution of divalent and trivalent cations. Accordingly, different models with or without partial (Cu, Mn) occupancies at Cu1 or Cu2, with different valences (Mn^{II}, Mn^{III}), or with a possible partial occupancy of K at the K1 and K2 sites were taken into account and comparative refinements have been carried out.

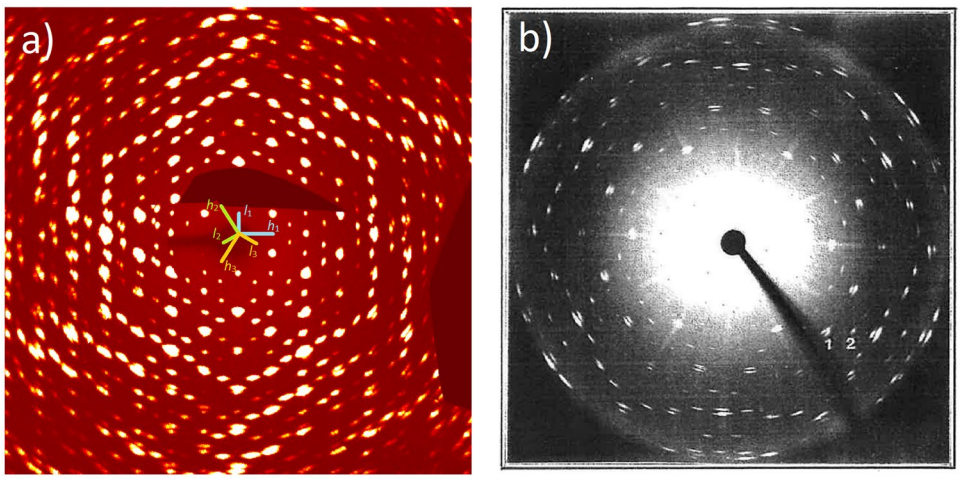

Fig. 2 **a** Reconstructed $h0l$ reciprocal lattice plane of $K[(Cu^{II},Mn^{II},Mn^{III})_2(TeO_3)_3]\bullet 2H_2O$, including reciprocal lattice vectors of the three twin domains. **b** Precession photograph of the same reciprocal plane recorded during the original investigation by Miletich (1993a)

Table 2 Selected interatomic distances in K[(Cu^{II},Mn^{II},Mn^{III})$_2$(TeO$_3$)$_3$]·2H$_2$O

Atoms	distance / Å	Atoms	distance / Å
Te1—O11	1.87(3)	Cu2|Mn2—O12	2.07(3)
Te1—O1	1.884(12)	Cu2|Mn2—O17	2.304(16)
Te1—O21^{i}	1.889(17)	Mn3—O6	1.88(2)
Te2—O6	1.86(2)	Mn3—O3	2.03(2)
Te2—O7	1.878(17)	Mn3—O1^{viii}	2.088(15)
Te2—O12	1.901(12)	Mn3—O9^{viii}	2.11(2)
Te3—O13	1.86(2)	Mn3—O2^{viii}	2.171(19)
Te3—O15^{ii}	1.900(18)	Mn3—O10	2.19(2)
Te3—O10	1.904(13)	Mn4—O11^{i}	1.90(3)
Te4—O16	1.88(2)	Mn4—O16^{i}	1.95(2)
Te4—O14^{i}	1.88(2)	Mn4—O17	2.018(15)
Te4—O17	1.886(13)	Mn4—O12	2.09(3)
Te5—O22	1.861(18)	Mn4—O18	2.181(19)
Te5—O18	1.878(12)	Mn4—O13	2.189(19)
Te5—O9^{i}	1.90(2)	K1—Ow5^{vi}	2.71(2)
Te6—O4^{iii}	1.82(2)	K1—Ow8	2.77(4)
Te6—O2i^{v}	1.907(12)	K1—Ow5	2.77(2)
Te6—O3^{iii}	1.93(2)	K1—Ow8^{viii}	2.78(4)
Cu1|Mn1—O22^{v}	1.929(18)	K1—O1	2.893(12)
Cu1|Mn1—O2^{vi}	1.966(18)	K1—O21^{i}	3.007(19)
Cu1|Mn1—O10^{vii}	2.03(2)	K1—O11	3.16(3)
Cu1|Mn1—O4	2.07(2)	K2—Ow19^{ii}	2.70(3)
Cu1|Mn1—O7	2.075(17)	K2—Ow20^{ix}	2.74(2)
Cu1|Mn1—O1^{vi}	2.311(15)	K2—Ow19^{ix}	2.75(3)
Cu2|Mn2—O15	1.923(18)	K2—Ow20	2.77(2)
Cu2|Mn2—O18	2.026(19)	K2—O10	2.932(13)
Cu2|Mn2—O21	2.033(18)	K2—O13	2.96(2)
Cu2|Mn2—O14	2.06(2)	K2—O15^{iii}	3.151(19)

Symmetry codes: (i) 1–*x*, 1/2+*y*, 1–*z*; (ii) *x*, 1+*y*, *z*; (iii) 1+*x*, *y*, *z*; (iv) 1+*x*, *y*, -1+*z*; (v) -1+*x*, *y*, *z*; (vi) -*x*, -1/2+*y*, 1–*z*; (vii) *x*, -1+*y*, *z*; (viii) -*x*, 1/2+*y*, 1–*z*; (ix) 1–*x*, 1/2+*y*, -*z*

The results of the final refinement are summarized in Table 1, positional parameters are provided in the cif file (*cf.* supplement material), and selected interatomic distances are listed in Table 2. Additional details can be found in the joint CCDC/FIZ Karlsruhe online deposition service: https://www.ccdc.cam.ac.uk/structures/ by quoting the deposition number given in Table 1. Graphical representations of the crystal structure were created with DIAMOND (Brandenburg 2016). As no other equivalent zemannite-type superstructure has been described as a reference phase, atom labels and coordinates were standardized with STRUCTURE-TIDY (Gelato and Parthé 1987).

Results and discussion

General aspects of the zemannite structure type

The zemannite structure type covers crystal structures of large compositional variability and can best be described with the general formula $A_{2-x}[M_2(TeO_3)_3]\cdot nH_2O$. *A* represents an alkali (Na^+, K^+) or alkaline earth metal (Mg^{2+}, Ba^{2+}) cation, while *M* accounts for a di- or trivalent first-row transition metal atom (*e.g.* Mn^{II}, Mn^{III}, Fe^{III}, Co^{II}, Ni^{II}, Zn^{II}). *M* can either be occupied exclusively by divalent metal cations, *e.g.* in $Na_2[Co_2(TeO_3)_3]\cdot 3H_2O$ and $Na_2[Zn_2(TeO_3)_3]\cdot 3H_2O$ (Miletich 1995b) or can represent a mixture of di- and trivalent cations, most commonly corresponding to the ratio 1:1. This is the case for the mineral zemannite itself, with composition $Mg_{0.5}[Zn^{II}Fe^{III}(TeO_3)_3]\cdot(4.5–n)H_2O$ (Miletich 1995a; Cametti et al. 2017; Missen et al. 2019b; Effenberger et al. 2023), but also for the isostructural minerals kinichilite ($Mg_{0.5}[(Mn^{II},Zn^{II})Fe^{III}(TeO_3)_3]\cdot 4.5H_2O$, Hori et al. 1981), ilirneyite ($Mg_{0.5}[Zn^{II}Mn^{III}(TeO_3)_3]\cdot 4.5H_2O$, Pekov et al. 2018) and keystoneite ($Mg_{0.5}Ni^{II}Fe^{III}(TeO_3)_3\cdot 4H_2O$, Missen et al. 2021). The variation of the valences of the *A* and *M* atoms results in the fact that different numbers of *A* atoms per formula unit (p.f.u.) can exist, with a variation range up to 2 cations p.f.u.. Even *A*-free phases, such as $Sc_2(SeO_3)_3$ (Wontcheu and Schleid 2003) and β-$Ga_2(TeO_3)_3$ (Kong et al. 2010), have been reported, thus exhibiting an "empty" zemannite-type structure.

The zemannite structure type consists of an anionic framework built up from trigonal-pyramidal [TeO_3] units and [M_2O_9] dimers of face-sharing octahedra. These groups are interconnected to the other type of building blocks by corner-sharing. The $[M_2(TeO_3)_3]^{y-}$ framework encloses large channels that are oriented along [001] of a hexagonal unit-cell ($a \approx 9.3$ Å, $c \approx 7.7$ Å), which has been described in either $P6_3/m$ or $P6_3$ space group symmetries. A most recent re-evaluation of the zemannite structure based on a natural sample revealed violations in the systematic absences corresponding to the 6_3 screw axis. The related structure refinements suggest *P*3 as the true space group symmetry of the archetype crystal structure (Effenberger et al. 2023).

Together with a variable amount of H_2O molecules, the *A* cations represent the extra-framework constituents distributed inside these topologically hexagonal channels. Depending on the amount of *A* cations present in the structure, the *A* cations are positioned either exactly at the central axis of the channels, such as exemplified in the structure of the mineral zemannite (Miletich 1995a). Alternatively, they are displaced at distances of up to ~2 Å off this central axis, due to the confined space inside the channel, in particular if the number or the size of *A* cations exceeds certain limits (*e.g.*

as in $Na_2[Co_2(TeO_3)_3]\cdot 3H_2O$, Miletich 1995b). In the latter case, the occupancies are usually modelled with ~$^1/_3$ for refinements in the parental hexagonal symmetry, which in fact represents only the symmetry of the framework but not that of the channel contents. Equivalent partial occupancies apply to the H_2O molecules, which in turn belong in most cases to the coordination spheres of hydrated *A* cations.

Lattice properties of the new $K[(Cu,Mn)_2(TeO_3)_3]\cdot 2H_2O$ zemannite

Considering the triplicate twinning along the pseudo-hexagonal axis in analogy to the parental 6/*m* Laue symmetry as shown in Fig. 2, the individual lattice domains follow monoclinic metrics with the diad aligned parallel to the hexagonal *c*-axis. Referring to a standard setting of the monoclinic diad being parallel to the *b* axis, the actual lattice can be described as a doubled zemannite structure (Fig. 3). The doubling occurs along [100], [010] or [$\bar{1}$10]. As [100] or its two symmetry-equivalent directions are three possible directions for doubling of the unit-cell, it is not surprising that threefold twinning was observed, following the lost rotation by each 120°. Accordingly, this threefold twinning leads to the formation of pseudo-sixfold symmetry in the diffraction pattern. The *a*:*c* ratio, which in case of an undistorted hexagonal lattice corresponds to 1:$\sqrt{3}$, clearly deviates with a ratio of 1:1.677 from metrical hexagonality. In addition, a small but significant deviation of β from ideal 90° confirms the observed lattice distortion, which is the reason why the three twin domains do not perfectly coincide, thus suggesting twinning by non-merohedry. This is manifested in reciprocal space in particular at higher *h* and *l* values as referring to the monoclinic unit-cell of $K[(Cu^{II},Mn^{II},Mn^{III})_2(TeO_3)_3]\cdot 2H_2O$. The remarkable shape of the diffraction pattern has already been noted during the original investigation (Fig. 2b, Miletich 1993a) and a unit-cell of $a = 18.54(5)$ Å, $b = 7.76(4)$ Å, $c = 9.39(4)$ Å, $\beta = 118.1(6)°$ as transferred to the standard monoclinic setting was derived at that time. Within the scope of the current study, we determined a similar unit-cell ($a = 9.3857(13)$ Å, $b = 7.6381(10)$ Å, $c = 15.746(2)$ Å, $\beta = 90.464(4)°$), which follows a different base-vector setting in order to achieve a monoclinic angle being close to 90°.

Crystallographic sites in the monoclinic superstructure

Compared to $Na_2[Co_2(TeO_3)_3]\cdot 3H_2O$ (Miletich 1995b) as a representative of the aristotype $P6_3/m$ symmetry, the crystal structure of $K[(Cu^{II},Mn^{II},Mn^{III})_2(TeO_3)_3]\cdot 2H_2O$ is subjected to a loss of the threefold rotation symmetry and the mirror plane perpendicular to the former sixfold axis of rotation. In addition, the doubling of the unit-cell causes the need for further symmetry-independent sites. This is manifested by the fact that the original eight atomic sites, some of which exhibit specific point symmetries, are now distributed over 34 independent sites, all of them corresponding to the general Wyckoff position 2 *a* in space group $P2_1$. The framework sites Te1 (site symmetry *m*..), Co1 (3..), O1 (*m*..) and O2 (1) in $P6_3/m$ are split into six Te, four *M* (two Cu and two Mn) and 18 O sites in the monoclinic superstructure. The Na1 site, which is only $^1/_3$ occupied in $Na_2[Co_2(TeO_3)_3]\cdot 3H_2O$, results in two fully occupied K sites, corresponding to only half the amount of *A* atoms p.f.u. compared to $Na_2[Co_2(TeO_3)_3]\cdot 3H_2O$. With respect to the H_2O sites O3, O4 and O5 in the parental hexagonal structure, the four Ow sites in $K[(Cu^{II},Mn^{II},Mn^{III})_2(TeO_3)_3]\cdot 2H_2O$, (viz. Ow5, Ow8, Ow19 and Ow20) are more or less equivalent to O3-type and, with some deviations, to O4-type

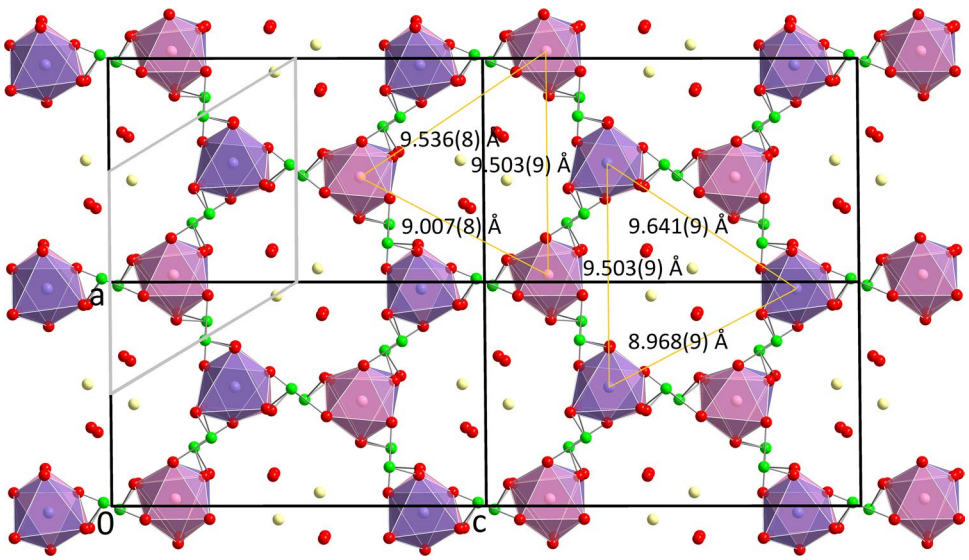

Fig. 3 The crystal structure of $K[(Cu^{II},Mn^{II},Mn^{III})_2(TeO_3)_3]\cdot 2H_2O$ in a projection along [0$\bar{1}$0]. Te atoms are drawn as green, K as yellow and O as red spheres. The Mn3 and Mn4 atoms are given in pink, those of (Cu,Mn)1 and (Cu,Mn)2 are depicted in purple. Octahedral coordination polyhedra are drawn for the *M* atoms. K—O bonds were omitted for clarity, and all atomic radii were fixed to a value of 0.25 Å. Grey lines mark the corresponding base cell of (pseudo)hexagonal zemannite. Yellow lines mark distances between (Cu,Mn) positions with the same *y*/*b* value

positions. The positions of H atoms related to the H_2O molecules could not be determined in the refinements.

Stereochemistry of the [TeO_3] groups and [M_2O_9] dimer units

The Te atoms are coordinated by three O atoms in a trigonal-pyramidal shape with the resulting [TeO_3] units being isolated from each other. The bond valence sums (BVS) of the Te atoms were calculated to 3.90 (Te1), 3.91 (Te2), 3.82 (Te3), 3.88 (Te4), 3.91 (Te5) and 3.90 (Te6) valence units (v.u., Brese and O'Keeffe 1991) based on the Te—O contacts given in Table 2. These values show good agreement with the ideal value of 4 as expected for an oxidotellurate(IV). The marginally smaller values originate from the presence of five additional O contacts for each Te site in the range of 2.8–3.5 Å, which have not been taken into account. Employing the revised parameters reported by Mills and Christy (2013), which require the consideration of all O contacts within 3.5 Å, the BVS values amount to 4.00 (Te1), 3.99 (Te2), 3.95 (Te3), 3.98 (Te4), 3.96 (Te5) and 4.01 (Te6) v.u. in almost perfect agreement with expectations.

The *M* sites are coordinated by six O atoms with distances ranging from 1.88(2) Å to 2.311(15) Å (Table 2) in a distorted octahedral shape. The distribution of individual *M*—O distances is very different for the Cu and Mn sites. The Cu-atoms are surrounded by five O contacts closer than 2.1 Å and a sixth O atom at a distance of slightly more than 2.3 Å, resulting in a [5 + 1]-like coordination. The Mn sites show a more uniform distribution of bond lengths, with the two longest contacts being at distances of almost 2.2 Å each. The [MnO_6] polyhedra can be described with a [4 + 2] or [2 + 2 + 2] coordination. The significant distortion of the [MO_6] octahedra is not surprising, because Cu^{II} (d^9) and Mn^{III} (d^4) atoms are known for their strong Jahn-Teller-effects (Lufaso and Woodward 2004).

The degree of octahedral distortion was analysed using OCTADIST (Ketkaew et al. 2021) and compared to the zemannite mineral phase $Mg_{0.5}[ZnFe(TeO_3)_3]\cdot4.5H_2O$ (Miletich 1995a) and the synthetic zemannite-type phase $Na_2[Co_2(TeO_3)_3]\cdot3H_2O$ (Miletich 1995b) (Table 3). The individual parameters referring to polyhedral distortion are (i) the average *M*—O distance d_{mean}, (ii) the distance distortion ζ, (iii) the angle distortion Σ, (iv) the tilting distortion Δ, and (v) the torsional distortion θ. Interestingly, the parameters cannot be used to make a clear distinction between the polyhedron types, although the distribution of bond lengths does (*cf.* Table 2). In comparison with $Mg_{0.5}[ZnFe(TeO_3)_3]\cdot4.5H_2O$, which exhibits no Jahn-Teller induced effect for Zn^{2+} and Fe^{3+}, similar values for most distortion parameters are revealed. Only the tilting distortion Δ shows significant differences. In contrast, synthetic $Na_2[Co_2(TeO_3)_3]\cdot3H_2O$ exhibits much more regular octahedra with consequently lower distortion parameters.

Table 3 Octahedral distortion parameters for the *M* sites in K[(Cu^{II},Mn^{II},Mn^{III})$_2$(TeO$_3$)$_3$]·2H$_2$O compared with the literature phases $Mg_{0.5}[ZnFe(TeO_3)_3]\cdot4.5H_2O$ (Miletich 1995a) and $Na_2[Co_2(TeO_3)_3]\cdot3H_2O$ (Miletich 1995b)

Site	d_{mean} / Å	ζ / Å	Δ	Σ / °	θ / °
(Cu,Mn)1	2.0637	0.5375	0.00356	53.51	139.70
(Cu,Mn)2	2.0695	0.4652	0.00304	71.61	164.12
Mn3	2.0782	0.4941	0.00250	76.13	149.46
Mn4	2.0549	0.5782	0.00275	66.92	148.59
*M*1 (Miletich 1995a)	2.0767	0.4055	0.00106	78.98	161.00
Co1 (Miletich 1995b)	2.1173	0.2967	0.00055	45.70	88.08

Apart from the fact that the *M* sites in these different representatives correspond to different point symmetries, one has to emphasize that octahedral distortion certainly is superimposed by two effects, which is on one hand the topologically induced distortion within the face-sharing dimers, and on the other hand the electronically induced Jahn-Teller effect.

Nevertheless, considering the *M*—O distances related by the former threefold symmetry, it clearly shows that an influence of the Jahn-Teller effect is present and is apparent for the origin of the symmetry reduction. If one compares the bond lengths to the three O atoms shared within the dimer, clear differences in the *M*—O distances can be seen: *e.g.* Cu2—O17 = 2.30(2) Å, Cu2—O18 = 2.03(2) Å, Cu2—O12 = 2.07(3) Å; Mn4—O17 = 2.02(2) Å, Mn4—O18 = 2.18(2) Å, Mn4—O12 = 2.09(3) Å within the [Cu2Mn4O_9] dimer. Short and long *M*—O bonds are arranged in a complementary fashion as it can be expected by the cooperative effect of the Jahn-Teller distortion in connection with balancing the bond valence contributions. While the bond valences of Te^{IV} in the [TeO_3] groups are remarkably close to the ideal values, the occupancy of the *M* positions can only be explained by a significant degree of substitution at any of the four *M* sites. The BVS as calculated for full occupancy with only Cu^{II}, Mn^{II} or Mn^{III} reveal significant over- or undersaturation for all four *M* sites, which necessitates a separate discussion of the occupancies.

(Cu^{II},Mn^{II},Mn^{III}) distribution at octahedrally coordinated M sites

Since the refinements of the sites corresponding to the extra-channel K^+ cations revealed full occupancy, each half of the *M* atoms within the framework must correspond to di- and trivalent transition-metal cations due to charge neutrality. Such a K[$M^{II}M^{III}$(TeO$_3$)$_3$]·2H$_2$O composition reflects an equivalent charge distribution as manifested by the distribution of $Zn^{II} + Fe^{III}$, $Mn^{II} + Fe^{III}$, $Ni^{II} + Fe^{III}$, and $Zn^{II} + Mn^{III}$ in the host frameworks of zemannite and the isostructural minerals (Miletich 1995a; Cametti et al. 2017; Missen et al. 2019b; Effenberger et al. 2023).

It therefore can be assumed that each [M_2O_9] dimer formed from two face-sharing [MO_6] octahedra hosts one divalent and one trivalent *M* atom. This assumption is supported by bond-valence considerations for the O atoms of the shared face, which is similar compared to the one discussed by Cametti et al. (2017). When refining in the higher-symmetric $P2_1/m$ space group, it is not possible to distinguish Cu and Mn sites due to identical environments caused by local mirror-plane symmetry. Lowering the symmetry to $P2_1$, the number of *M* sites doubles from two to four, and each [M_2O_9] dimer now encompasses two different *M* sites. Of these two, one exhibits a notably higher electronic density and therefore was assigned to be preferentially occupied by Cu atoms. Accordingly, non-centrosymmetric $P2_1$ was ultimately chosen as the space group, despite the more problematic refinement (such as evidenced by the strong correlation effects, negative ADPs and non-convergence of *y/b*-related parameters of distinct atoms). The alternative structure model in $P2_1/m$ is attached in the supplementary materials.

Refining the relative occupancies of Cu and Mn atoms at the same site, a Cu:Mn ratio of 0.35(2):0.65(2) was obtained in $P2_1/m$, which significantly differs from equal amounts of Cu and Mn. Refinements in $P2_1$ yield occupancies of Cu:Mn of 0.73(3):0.27(3) on average for the (Cu,Mn)1 and (Cu,Mn)2 positions, while the Mn3 and Mn4 sites exclusively host Mn atoms. This is in good agreement with the results of the preliminary SEM–EDX investigations reported by Miletich (1993a), who suggested a $K_{1.02}[(Mn_{0.60}Cu_{0.40})_2(TeO_3)_3]\cdot nH_2O$ composition thus showing significant excess of Mn relative to Cu contents p.f.u.. Considering the most likely valence variations of Mn and Cu atoms, one can consider Mn to be both di- and trivalent (Mn^{II}, Mn^{III}), whereas the Cu atoms only appear reasonable in the divalent state (Cu^{II}). If all Mn atoms would be present in the form of trivalent Mn^{III}, a reduction of the K-content in order to balance charges is necessary. However, when freely refining the occupancies of the two K sites, the s.o.f.s account for 0.934(14) on average, which does not correlate with the magnitude of the Mn excess. This, in turn, suggests that the ratio between divalent and trivalent cations indeed is close to 1:1, and therefore Mn^{II} and Mn^{III} atoms must coexist.

Further information on the occupational distribution of atoms at the *M* sites can be derived by evaluating the bond valences, as calculated for the (Cu,Mn)1, (Cu,Mn)2, Mn3 and Mn4 sites in variations of exclusive occupancy through Cu^{II}, Mn^{II}, and Mn^{III} (Table 4). It turns out that exclusive occupancies with only divalent or trivalent cations result in a respective oversaturation (for Mn^{II} and Cu^{II}) or undersaturation (for Mn^{III}) of the total bond strength for all *M* sites. Consequently, the *M* sites must show mixed occupancy. A distribution of $Cu^{II}_{1-x}Mn^{III}_{x}$ (*M*1, *M*2) and $Mn^{II}_{x}Mn^{III}_{1-x}$ (*M*3, *M*4) was chosen over that of $Cu^{II}_{1-x}Mn^{II}_{x}$ (*M*1, *M*2) and Mn^{III} (*M*3, *M*4) due to the sizes of the *M*1 and *M*2 sites. The mixed bond valences calculated with Eq. 2 by Bosi (2014) for cases of $Cu^{II}_{0.73}Mn^{III}_{0.27}$ and $Cu^{II}_{0.73}Mn^{II}_{0.27}$ at the *M*1 and *M*2 sites (Table 4) support this assumption. The potential presence of both Mn^{II} and Mn^{III} besides Cu^{II} at the *M*1 and *M*2 sites was considered as well. However, this led to a worse agreement of the mixed bond valences with the corresponding charge of the sites than a mixed occupancy with just Mn^{III} besides Cu^{II}.

Additionally, the ideal proportions for a partial Mn^{III}/Cu^{II} occupancy were determined independently from the ratios obtained by the refinement but based on the respective extent of over- or undersaturation of the bond valences Δ_{BV} ($\Delta_{BV} = |BV_{actual} - BV_{ideal}|$). Using the approximations of

$$x = \frac{\Delta_{BV}(Mn^{III})}{\Delta_{BV}(Mn^{III}) + \Delta_{BV}(Cu^{II})}$$

for *M*1 and *M*2 and

$$x = \frac{\Delta_{BV}(Mn^{II})}{\Delta_{BV}(Mn^{II}) + \Delta_{BV}(Mn^{III})}$$

for *M*3 and *M*4, values of $0.14 \leq x \leq 0.50$ were obtained (Table 4). These values lead to a composition of $K[(Cu^{II}_{0.28}Mn^{II}_{0.11}Mn^{III}_{0.61})_2(TeO_3)_3]\cdot 2H_2O$, which corresponds satisfactorily with the refined composition of $(K[(Cu_{0.35}Mn_{0.65})_2(TeO_3)_3]\cdot 2H_2O$, for $P2_1/m$ and $K[(Cu_{0.37}Mn_{0.63})_2(TeO_3)_3]\cdot 2H_2O$, for $P2_1$), and ultimately is also in good agreement with the original composition ($K_{1.02}[(Cu_{0.40}Mn_{0.60})_2(TeO_3)_3]\cdot nH_2O$) determined by means of EDX data (Miletich 1993a).

Distribution of extra-framework K^+ ions and H_2O molecules

The distribution of the extra-framework constituents within the topological channels offers a comparatively

Table 4 Bond valence sums / v.u. of the *M*1, *M*2, *M*3 and *M*4 sites as derived from empirical bond-valence parameters given by Brese and O'Keeffe (1991)

Site	Cu^{II}	Mn^{II}	Mn^{III}	$Cu^{II}_{0.73}Mn^{II}_{0.27}$	$Cu^{II}_{0.73}Mn^{III}_{0.27}$	$Cu^{II}_{1-x}Mn^{III}_{x}$	$Mn^{II}_{x}Mn^{III}_{1-x}$
(Cu,Mn)1	2.23	3.01	2.77	2.44 (2.00)	2.38 (2.27)	2.50 (x=0.50)	-
(Cu,Mn)2	2.18	2.95	2.72	2.39 (2.00)	2.33 (2.27)	2.39 (x=0.39)	-
Mn3	2.13	2.87	2.65	2.65 (3.00)	2.71 (2.73)	-	2.71 (x=0.29)
Mn4	2.27	3.06	2.83	2.83 (3.00)	2.89 (2.73)	-	2.86 (x=0.14)

Values were determined for exclusive occupation by Cu^{II}, Mn^{II}, and Mn^{III} and compositions of $Cu^{II}_{0.73}Mn^{III}_{0.27}$ and $Cu^{II}_{0.73}Mn^{II}_{0.27}$ (charge of the site in parentheses). For mixed occupation corresponding to $Cu^{II}_{1-x}Mn^{III}_{x}$ and $Mn^{II}_{x}Mn^{III}_{1-x}$ substitutions, the determined substitution x is given in parentheses instead

clear picture. The K positions are displaced off the central axis of the channels at a distance of 1.04 Å (K1) and 1.06 Å (K2). The smaller distances from the central axis seem plausible considering that only half as many cations need to be accommodated within the channel compared to $Na_2[Co_2(TeO_3)_3]\cdot 3H_2O$ (Miletich 1995b). The K atoms are coordinated by seven O atoms in a range of 2.7–3.2 Å (Table 2). Three of the neighbouring O atoms belong to the anionic framework, while the other four belong to H_2O molecules, corresponding to the Ow5, Ow8, Ow19 and Ow20 sites. The presence of H_2O molecules at these sites is indicated by their otherwise low BVS (Brown 2002) of in total 0.37–0.42 v.u. as derived from the parameters given by Brese and O'Keeffe (1991). The $[KO_7]$ polyhedra are interconnected through shared edges and form zig-zag chains along the [001] axis (Fig. 4). The total BVS of the K sites considering both the framework- and the H_2O-O atoms was calculated to values of 1.02 (K1) and 1.06 v.u. (K2), which in turn perfectly matches the theoretical value for a monovalent cation. Upon now, all zemannite-type structures, which have *A* cations not located directly at the centre of the channels, were modelled with a disorder of at least a part of the *A* cations. $K[(Cu^{II},Mn^{II},Mn^{III})_2(TeO_3)_3]\cdot 2H_2O$ thus is the first zemannite-type structure reported with fully ordered off-center displaced *A* cations inside the channels.

The unidirectional presence of K^+ cations and H_2O molecules in the channels is apparently crosslinked with the distortion of the surrounding framework, as manifested by the lattice parameters and the significant difference of the *c*/*a* ratio from ideal $\sqrt{3}$ as discussed previously. The channels have their smallest diameter along the direction corresponding to the section, within which the K atoms are displaced from the central channel axis. Since the H_2O molecules are further away from the central axis (1.63–1.73 Å) and require a correspondingly larger amount of space for getting accommodated, the channel diameter is larger in those directions.

The distances between the second closest *M* positions in Fig. 3 (marked with yellow lines) show variations of more than 0.6 Å (8.878(7)–9.532(7) Å), thus demonstrating the deviation from a strict hexagonal symmetry of the channels. When looking at the cross section, the pseudohexagonal channels have an elliptically elongated shape and are stacked next to each other in a herringbone-like pattern with only two out of three possible channel distortions being realized within a single domain. The arrangement of the deformed channels can finally be understood as the origin of the existing superstructure.

Distortions of the channels from the superordinate hexagonal symmetry have been observed for several other zemannite-type phases. In the crystal structures of $Ba[M_2(SeO_3)_3]\cdot 3H_2O$ (M = Co, Mn, Mg) (Johnston and Harrison 2011), which exhibit a fourfold zemannite superstructure obtained by doubling **a** and **b** of the parent zemannite unit-cell, the $M\cdots M$ distances as drawn in Fig. 3 vary by only a maximum of 0.15 Å compared to more than 0.6 Å for $K[(Cu^{II},Mn^{II},Mn^{III})_2(TeO_3)_3]\cdot 2H_2O$. This can be easily understood as Co^{II}, Mn^{II} and Mg^{II} reveal no Jahn-Teller effect compared to the pronounced polyhedral distortions known for Mn^{III} and Cu^{II}. The recently discovered phases $Rb_{1.5}[(Mn^{II},Mn^{III})_2(TeO_3)_3]\cdot 1.25H_2O$ and $Cs[(Mn^{II},Mn^{III})(TeO_3)_3]\cdot H_2O$ (Eder et al. 2023) also exhibit such a fourfold superstructure, with the channels widening up in the direction of the *A* cations due to the lower crystal water content and the higher off-center displacement of the larger Rb^+ and Cs^+ cations. Together with the presence of Jahn-Teller-active

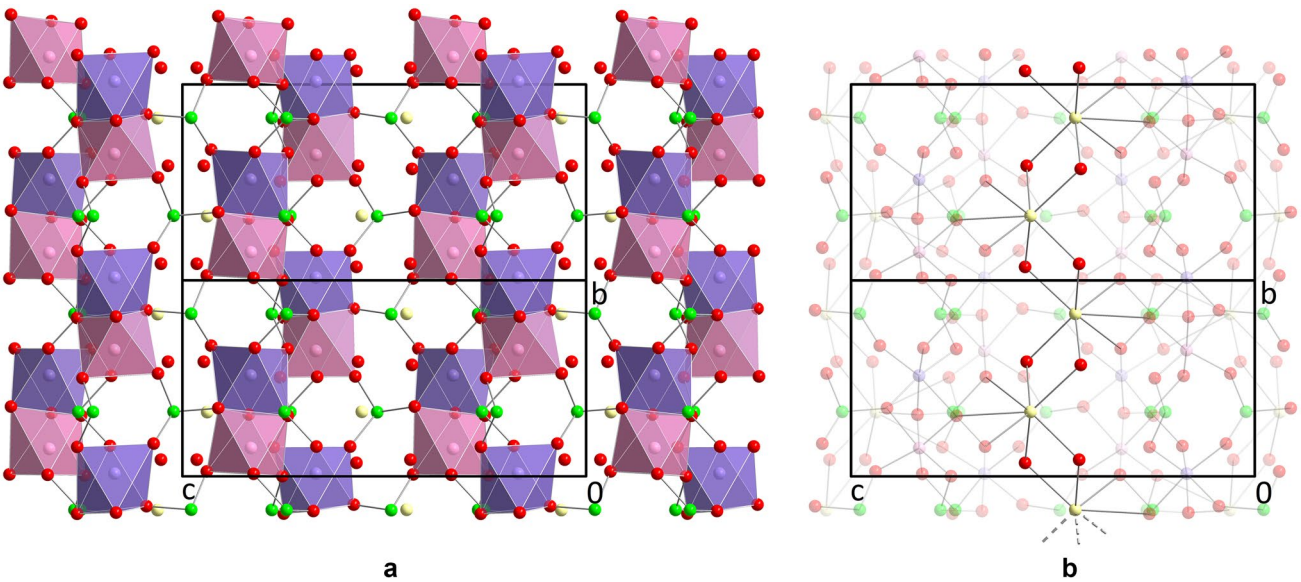

Fig. 4 The crystal structure of $K[(Cu^{II},Mn^{II},Mn^{III})_2(TeO_3)_3]\cdot 2H_2O$ in a projection along $[\bar{1}00]$. Colour codes and atomic radii refer to Fig. 2. **a** K—O-bonds were omitted for clarity. **b** Coordination of K^+ cations inside the channels with all framework atoms drawn in transparent colours

Mn^{III} within the framework, the larger *A* cations inside the channels lead to increased distortions of the channels with differences in the corresponding *M*···*M* distances (as drawn in yellow in Fig. 3) ranging up to ~ 1.5 Å.

Conclusion and outlook

The crystal structure of $K[(Cu^{II},Mn^{II},Mn^{III})_2(TeO_3)_3]\cdot 2H_2O$ was solved about 30 years after its synthesis. It is the first zemannite-type phase that was solved and refined with monoclinic space group symmetry, which exhibits a twofold superstructure relative to the usual hexagonal zemannite base cell. The symmetry reduction and distortion of the framework is caused by the Jahn-Teller-distortion of octahedrally coordinated Cu^{II} and Mn^{III} cations at the *M* sites within the framework and includes twinning of individual monoclinically distorted crystal domains following the superordinate hexagonal symmetry. Refinements of s.o.f.s and the evaluation of bond valences suggest a distribution of di- and trivalent cations at the octahedral *M* sites to approximate a ratio of 1:1 for the cation distribution $(Cu^{II}+Mn^{II}):Mn^{III}$. The excess of Mn was confirmed in each of the analyses performed and matches previous data reported by Miletich (1993a). From arguments about the cation size and the individual BVS, a distribution of $Cu^{II}_{1-x}Mn^{III}_{x}$ and $Mn^{II}_{x}Mn^{III}_{1-x}$ at each two of the four *M* positions can be assumed with a presumed *x* between ~ 0.14 and ~ 0.50. Based on the refinement of mixed Cu/Mn occupancies in $P2_1$, *x* was determined to 0.27(3).

A much clearer view is given for the structural arrangement within the channels. $K[(Cu^{II},Mn^{II},Mn^{III})_2(TeO_3)_3]\cdot 2H_2O$ represents the first zemannite-type phase with completely ordered extra-framework atoms where the *A* cations are not located at the central axis of the channels. The interaction between the off-center displaced guest constituents K^+ and H_2O and the channel walls leads to a cooperative distortion of the channels, the herringbone-like arrangement of which is responsible for the superstructure. During our current research on novel zemannite-type oxidotellurate(IV) phases, we found two further zemannite-type phases exhibiting a twofold superstructure with similar metrics, viz. $K_2[Cu_2(TeO_3)_3]\cdot 2H_2O$ and $K_2[Co_2(TeO_3)_3]\cdot 2.5H_2O$ (Eder et al. 2023). The latter also exhibits an incommensurate modulation along the reciprocal direction parallel to the channel axis.

A reproducible synthesis of the title compound obtained 30 years ago proved to be very difficult, not only because the reported fluid loss within the hydrothermal experiment is quite difficult to control, but also because the variable (Cu,Mn) ratio was at that time deliberately used for the synthesis of the of the Cu-substituted denningites. Although inserting only starting materials with Mn in the divalent state, redox reactions within the hydrothermal fluid is known to produce Mn^{III}-bearing reaction products, as even manifested through recent investigations on phases in the system $Mn^{II}O$-$Te^{IV}O_2$ (Eder and Weil 2022). During attempts to reproduce K-(Cu,Mn) phases, we indeed obtained zemannite-type phases, apparently with a twofold superstructure, but not exhibiting such a strong distortion of the unit-cell. In addition, a phase exhibiting a rhombohedral threefold superstructure has also been obtained. For both phases, the exact Cu:Mn ratio is yet unknown, but they are believed to be richer in Cu than the $K[(Cu^{II},Mn^{II},Mn^{III})_2(TeO_3)_3]\cdot 2H_2O$ title compound described in the current study. One of the investigated new Cu-containing zemannites even transformed from the rhombohedral to a threefold twinned monoclinic superstructure after ~2 h under the stream of dry nitrogen at room temperature. This suggests that the H_2O content certainly influences the occurrence of superstructures in zemannite-type phases. We recently observed an influence of the crystal water content on the superstructure formation for several other novel zemannite-type phases (Eder et al. 2023) as well, which offers various possibilities for further investigations on the tuning of different zemannite-type (super)structures.

Supplementary Information The online version contains supplementary material available at https://doi.org/10.1007/s00710-022-00808-9.

Acknowledgements This article is dedicated to Prof. Josef Zemann (1923-2022) on the occasion of the 100th anniversary of his birthday. Constructive reviews by two anonymous experts and comments by editor Thomas Armbruster and editor-in-chief Lutz Nasdala are gratefully acknowledged. The X-ray centre of the Technical University of Vienna is acknowledged for providing access to the single-crystal diffractometer.

Funding Open access funding provided by TU Wien (TUW).

Availability of data sets CIF-files of the refinement in $P2_1$ and the alternative model in $P2_{1/m}$ can be obtained from the CCDC/FIZ Karlsruhe online deposition service: https://www.ccdc.cam.ac.uk/structures/ by quoting the deposition numbers 2216656 and 2216464, respectively.

References

Bosi F (2014) Bond valence at mixed occupancy sites. I Regular Polyhedra Acta Crystallogr B70:864–870

Brandenburg K (2016) Diamond (Version 4.0). Crystal and Molecular Structure Visualization

Brese NE, O'Keeffe M (1991) Bond-valence parameters for solids. Acta Crystallogr B47:192–197

Brown ID (2002) The Chemical Bond in Inorganic Chemistry: The Bond Valence Model. Oxford University Press, Oxford

Bruker (2021a) APEX-4. Bruker AXS Inc, Madison, Wisconsin, USA

Bruker (2021b) SAINT. Bruker AXS Inc, Madison, Wisconsin, USA

Cametti G, Churakov S, Armbruster T (2017) Reinvestigation of the zemannite structure and its dehydration behavior: a single-crystal X-ray and atomistic simulation study. Eur J Mineral 29:53–61

Cooper MA, Hawthorne FC (1996) The crystal structure of spiroffite. Canad Mineral 34:821–826

Eder F, Weil M (2022) Phase formation studies and crystal structure refinements in the Mn^{II}/Te^{IV}/O/(H) system. Z Anorg Allg Chem 648:e202200205. https://doi.org/10.1002/zaac.202200205

Eder F, Marsollier A, Weil M (2023) Structural studies on synthetic $A_{2-x}[M_2(TeO_3)_3]\cdot nH_2O$ (A = Na, K, Rb, Cs; M = Mn, Co, Ni, Cu, Zn) with zemannite-type structures. Miner Petrol. https://doi.org/10.1007/s00710-023-00814-5 (this issue)

Effenberger HS, Ende M, Miletich R (2023) New insights into the crystal chemistry of zemannite: Trigonal rather than hexagonal symmetry due to ordering within the host-guest structure. Miner Petrol https://doi.org/10.1007/s00710-023-00820-7 (this issue)

Gattow G, Zemann J (1958) Neubestimmung der Kristallstruktur von Azurit Cu$_3$(OH)$_2$(CO$_3$)$_2$. Acta Crystallogr 11:866–872

Gelato LM, Parthé E (1987) STRUCTURE TIDY - a computer program to standardize crystal structure data. J Appl Cryst 20:139–143

Hanke K, Kupcik V, Lindquist O (1973) The crystal structure of CuTe$_2$O$_5$. Acta Crystallogr B 29:963–970

Hori H, Koyama E, Nagashima K (1981) Kinichilite, a new mineral from the Kawazu mine, Shimoda city. Japan Mineral J 10(7):333–337

Johnston MG, Harrison WTA (2011) New BaM$_2$(SeO$_3$)$_3$·nH$_2$O (M= Co, Ni, Mn, Mg; n≈3) Zemannite-Type Frameworks: Single-Crystal Structures of BaCo$_2$(SeO$_3$)$_3$·3H$_2$O, BaMn$_2$(SeO$_3$)3·3H$_2$O and BaMg$_2$(SeO$_3$)$_3$·3H$_2$O. Eur J Inorg Chem. https://doi.org/10.1002/ejic.201100344

Ketkaew R, Tantirungrotechai Y, Harding P, Chastanet G, Guionneau P, Marchivie M, Harding DJ (2021) OctaDist: A Tool for Calculating Distortion Parameters in Spin Crossover and Coordination Complexes. Dalton Trans 50:1086–1096

Kong F, Xu X, Mao JG (2010) A Series of New Ternary and Quaternary Compounds in the Li^{I}-Ga^{III}-Te^{IV}-O System. Inorg Chem 49:11573–11580

Krause L, Herbst-Irmer R, Sheldrick GM, Stalke D (2015) Comparison of silver and molybdenum microfocus X-ray sources for single-crystal structure determination. J Appl Cryst 48:3–10

Lufaso MW, Woodward PM (2004) Jahn-Teller distortions, cation ordering and octahedral tilting in perovskites. Acta Crystallogr B 60:10–20

Mandarino JA, Matzat E, Williams SJ (1969) Zemannite, a new tellurite mineral from Moctezuma, Sonora, Mexico. Can Mineral 10:139–140

Matzat E (1967) Die Kristallstruktur eines unbenannten zeolithartigen Tellurminerals, {(Zn, Fe)$_2$[TeO$_3$]$_3$}Na$_x$H$_{2-x}$·yH$_2$O. Tschermaks Miner Petrogr Mitt 12:108–117

Miletich R (1993a) Kristallchemische Untersuchungen an natürlichen und synthetischen Telluriten mit zeolithartigen Kristallstrukturen. Dissertation, University of Vienna

Miletich R (1993b) Copper-substituted manganese-denningites, Mn(Mn$_{1-x}$Cu$_x$)(Te$_2$O$_5$)$_2$ ($0 \le x \le 1$): Synthesis and crystal chemistry. Miner Petrol 48:129–145

Miletich R (1995a) Crystal chemistry of the microporous tellurite minerals zemannite and kinichilite, Mg$_{0.5}$ (Me^{2+}Fe^{3+}(TeO$_3$)$_3$)·4.5H$_2$O, (Me^{2+}=Zn; Mn). Eur J Mineral 7:509–523

Miletich R (1995b) The synthetic microporous tellurites Na$_2$[Me_2(TeO$_3$)$_3$]·3H$_2$O (Me=Zn, Co): Crystal structure, De- and rehydration, and ion exchange properties. Monatsh Chem 126:417–430

Mills SJ, Christy AG (2013) Revised values of the bond-valence parameters for Te^{IV}–O, Te^{VI}–O and Te^{IV}–Cl. Acta Crystallogr B 69:145–149

Missen OP, Mills S, Spratt J (2019a) Crystal chemistry of zemannite-type structures: II. Synthetic Sodium Zemannite Eur J Mineral 31:529–536

Missen OP, Mills S, Spratt J, Birch WD, Brugger J (2019b) Crystal chemistry of zemannite-type structures: I. A re-examination of zemannite from Moctezuma. Mexico Eur J Mineral 31:519–527

Missen OP, Back M, Mills S, Roberts A, LePage Y, Pinch W, Mandarino J (2021) Crystal Chemistry of Zemannite-type structures: III. Keystoneite, the Ni^{2+}-analogue of zemannite, and ferrotellurite discredited. Can Mineral 59:355–364

Pekov IV, Siidra OI, Vlasov EA, Yapaskurt VO, Polekhovsky YS, Apletalin AV (2018) Ilirneyite, Mg$_{0.5}$[ZnMn^{3+}(TeO$_3$)$_3$]·4.5H$_2$O, a New Mineral from Chukotka, Russia. Can Mineral 56(6):913–921

Sheldrick GM (2015a) SHELXT - Integrated space-group and crystal-structure determination. Acta Crystallogr A 71:3–8

Sheldrick GM (2015b) Crystal structure refinement with SHELXL. Acta Crystallogr C 71:3–8

Trömel M, Schmid D (1972) Tellurite des zweiwertigen Mangans, Kobalts und Nickels. Z Anorg Allg Chem 387(2):230–240

Walitzi EM (1965) Die Kristallstruktur von Denningit, (Mn, Ca, Zn) Te$_2$O$_5$. Ein Beispiel für die Koordination um vierwertiges Tellur. Tschermaks Miner Petrogr Mitt 10:241–255

Wildner M (1993) Zemannite-type Selenites: Crystal structures of K$_2$[CO$_2$(SeO$_3$)$_3$] · 2H$_2$O and K$_2$[Ni$_2$(SeO$_3$)$_3$] · 2H$_2$O. Miner Petrol 48:215–225

Wontcheu J, Schleid T (2003) Sc$_2$Se$_3$O$_9$: Scandium(III) Oxoselenate(IV) According to Sc$_2$[SeO$_3$]$_3$ with a Hexagonal "Lone-Pair" Channel Structure. Z Anorg Allg Chem 629(9):1463–1465

Zemann J (1968) The crystal chemistry of the tellurium oxide and tellurium oxosalt minerals. Z Kristallogr 127:315–326

Zemann J (1971) Zur Stereochemie des Te(IV) gegenüber Sauerstoff. Monatsh Chemie 102:1209–1216

Zemann J (1974) Tellurium. 52-A. Crystal chemistry. In: Wedepohl KH (ed) Handbook of Geochemistry, vol II/4. Springer, Berlin Heidelberg New York, p 5